

## Supplementary Information

V. Subbiah, T. Shen, M. Tetzlaff, A. Weissferdt, L. A. Byers, T. Cascone, A. Behrang, Meric-Bernstam, B. H. M. Mooers, S. M. Rothenberg, K. Ebata, and J. Wu

### **Patient-driven discovery and post-clinical validation of NTRK3 fusion as an acquired resistance mechanism to selpercatinib in RET fusion-positive lung cancer**

#### **Patient details**

A 62-year-old man with a one year past smoking history developed a dry hacking cough. He was evaluated by his primary physician and a chest X-ray was performed, which revealed soft tissue fullness in the right suprahilar area. A computerized tomography (CT) scan of the chest revealed a poorly defined spiculated-mass adjacent to the right hilum and mediastinum which severely narrowed the right upper lobe bronchus. The mass was approximately 4 cm and contiguous with a 1.4-cm lymph node in the right azygous area. There was also a 2-cm subcarinal lymph node. Metastatic disease in the liver was noted on the CT as well as porta hepatis lymphadenopathy. The patient subsequently came to the MD Anderson Cancer Center for further evaluation and treatment. CT of the abdomen and pelvis revealed multiple metastases visualized throughout the liver. There were enlarged porta hepatis lymph nodes and peripancreatic lymph nodes. A portacaval node measured 3 cm. Soft tissue densities were also identified in the mesentery suggesting peritoneal deposits. In addition, there were punctate calcifications noted in the mesentery. Magnetic resonance imaging (MRI) of the brain revealed approximately 30 subcentimeter intracranial metastases. A few of the lesions were associated

with a small amount of edema specifically in the right medial parietal lobe, the right lateral parietal lobe, the left posterior medial temporal lobe and the left posterior pons.

The patient underwent biopsy of a skin lesion in the left scapular area. Surgical pathology revealed high-grade neuroendocrine carcinoma of thoracic origin (Figure 1). A positron emission tomography (PET)/CT showed multiple hypermetabolic lesions in the right upper lung, liver, mesenteric lymph node, and extensively in the bones and the left posterior shoulder consistent with seeding of high-grade neuroendocrine carcinoma. Molecular profiling of tumor tissue from the left scapula area using the OncoMine® NGS platform revealed a *PTEN:c.723del p.F241fs\*15* Exon 7 deletion frameshift aberration. Immunohistochemical analysis for PD-L1 (*clone 22C3, Dako*) showed complete absence of membranous staining.

The patient received whole brain radiation of 3,000 cGy in 10 fractions for greater than 30 brain metastases. Following radiation, chemotherapy with carboplatin and etoposide IV Q 3 weeks and IV zoledronic acid was initiated (Figure 2A). Post 5 cycles patient's imaging evaluation showed progression in the lungs and liver (Figure 2B). The patient developed right lung collapse with moderate pleural effusion and ascites. He had anorexia, abdominal fullness, ageusia, nausea, over 20 pounds weight loss since diagnosis and required 2 L of oxygen to keep saturations above 95%. Serum bilirubin was elevated [total bilirubin: 3.3 (normal range: 0.2-1.3); direct: 2.6 mg/dL (normal range: 0.0-0.4)] (Figure 2C). Molecular analysis of cell-free DNA (cfDNA) with the Guardant360® test revealed *KIF5B-RET* fusion (variant allele frequency [VAF] 8.4%) and *PTEN F241fs* mutation (VAF 17.8%). He was then screened and enrolled on the selpercatinib (LOXO-292) LIBRETTO-001 trial (NCT03157128).

### **Next-generation sequencing (NGS) of tumor tissues and cfDNA**

Tumor biopsies were analyzed by NGS using the targeted TruSight® Tumor 170 (TST-170) panel from Illumina, which detects variants, amplifications, fusions, and splice variants of 170 genes related to solid tumor progression.<sup>1</sup> cfDNA was analyzed using the CLIA-certified

Guardant360 test<sup>2</sup> either with samples sent from the MD Anderson Cancer Center or with batch central testing by Loxo Oncology from serial cfDNA collection.

### **Cell culture experiments**

A His-tagged KHDRBS1-NTRK3 coding cDNA (Supplementary Figure S3) was chemically synthesized. BaF3 cells containing KIF5B-RET (BaF3/KIF5B-RET, KR) cells were reported previously.<sup>3,4</sup> BaF3/KHDRBS1-NTRK3 (KN) cells were made by infecting BaF3 cells with retrovirus encoding the His-tagged KHDRBS1-NTRK3 coding sequence and selecting for dual G418-resistant and IL-3-independent cells. BaF3/KIF5B-RET/KHDRBS1-NTRK3 (KRKN) cells were made by infecting BaF3/KHDRBS1-NTRK3 cells with lentivirus encoding KIF5B-RET. Cell viability assay for IC<sub>50</sub> determination and immunoblotting analyses were performed as described.<sup>4</sup>

For the pulldown of the His-tagged KHDRBS1-NTRK3 protein with Ni-NTA magnetic agarose beads, cells were lysed in RIPA buffer (150 mM NaCl, 1% NP-40, 0.5% deoxycholate, 0.1% SDS, 50 mM Tris;HCl, pH8.0) plus 1 mM dithiothreitol, 1 mM sodium vanadate, 20 mM *p*-nitrophenyl phosphate, 2 µg/ml aprotinin, 2 µg/ml leupeptin, and 1 mM phenylmethylsulfonyl fluoride. Cell lysates were sonicated. Cleared cell lysate supernatants (500 µg/each) were used for the pulldown of the His-tagged KHDRBS1-NTRK3 using the Ni-NTA magnetic beads following the supplier's (ThermoFisher Scientific, Waltham, MA, USA) instruction. The pulldown proteins were analyzed by immunoblotting.

Antibodies to phospho-TrkC(Tyr516) and TrkC was from ThermoFisher Scientific. Antibodies to phospho-RET(Tyr905), phospho-ERK1/2(Thr202/Tyr204), phospho-AKT(Ser473), and cleaved PARP(Asp214) were from Cell Signaling Technology (Danvers, MA, USA). The anti-Flag-tag (M2) antibody was from Sigma. Antibodies to ERK1/2 and AKT were from Santa Cruz Biotechnology (Dallas, TX, USA).

## Supplementary References

- 1 Na K, Kim HS, Shim HS et al. Targeted next-generation sequencing panel (TruSight Tumor 170) in diffuse glioma: a single institutional experience of 135 cases. *J Neurooncol* 2019;142:445-454.
- 2 Lanman RB, Mortimer SA, Zill OA et al. Analytical and Clinical Validation of a Digital Sequencing Panel for Quantitative, Highly Accurate Evaluation of Cell-Free Circulating Tumor DNA. *PLoS One* 2015;10:e0140712.
- 3 Huang Q, Schneeberger VE, Luetke N et al. Preclinical Modeling of KIF5B-RET Fusion Lung Adenocarcinoma. *Mol Cancer Ther* 2016;15:2521-2529.
- 4 Subbiah V, Shen T, Terzyan SS et al. Structural basis of acquired resistance to selipratinib and pralsetinib mediated by non-gatekeeper RET mutations. *Ann Oncol* 2021;32:261-268.

**Table S1.** Results of serial cfDNA analysis.

Cycle	Collection Date	Variant_type	Indel_type	Gene	Chromosome	Position	Exon	Mut_aa	Mut_nt	Mut_cdna	Transcript	Percentage	Fusion_gene_b	Fusion_position_a	Fusion_position_b	Direction_a	Direction_b	Downstream_gene	Copy_number
Screening	20-NOV-2017	Indel	Deletion	PTEN	10	89717695	7	p.Phe241fs	CT>C	c.723delT	NM_000314.4	37.19							
Screening	20-NOV-2017	Fusion		RET	10							16.32	KIF5B	43610190	32316459	1	1	A	
Screening	20-NOV-2017	CNV		EGFR															2.4082048
Cycle 01 Day 15	05-DEC-2017	SNV		EGFR	7	55231450	14	N552K	C>A	c.1656C>A	NM_005228.3	0.123667							
Cycle 01 Day 15	05-DEC-2017	Indel	Deletion	PTEN	10	89717695	7	p.Phe241fs	CT>C	c.723delT	NM_000314.4	0.88							
Cycle 01 Day 15	05-DEC-2017	Fusion		RET	10							0.283	KIF5B	43610190	32316459	1	1	A	
Cycle 03 Day 01	18-JAN-2018	SNV		EGFR	7	55231450	14	N552K	C>A	c.1656C>A	NM_005228.3	0.11							
Cycle 03 Day 01	18-JAN-2018	Indel		PTEN	10	89717695	7	F241fs	CT>C	c.723delT	NM_000314.4	0.29							
Cycle 03 Day 01	18-JAN-2018	Fusion		RET	10							0.18	KIF5B	43610190	32316459	1	1	A	
Cycle 05 Day 01	13-MAR-2018	Indel		PTEN	10	89717695	7	F241fs	CT>C	c.723delT	NM_000314.4	0.29							
Cycle 05 Day 01	13-MAR-2018	Fusion		RET	10							0.41	KIF5B	43610190	32316459	1	1	A	
Cycle 11 Day 01	04-SEP-2018	Indel	Deletion	PTEN	10	89717695	7	F241fs	CT>C	c.723delT	NM_000314.4	66.63							
Cycle 11 Day 01	04-SEP-2018	CNV		CDK6	7														3.01878
Cycle 11 Day 01	04-SEP-2018	CNV		EGFR	7														2.933789
Cycle 11 Day 01	04-SEP-2018	Fusion		RET	10							16.56	KIF5B	43610190	32316459	1	1	A	
On Study Progression	05-OCT-2018	Indel	Deletion	PTEN	10	89717695	7	F241fs	CT>C	c.723delT	NM_000314.4	70.21							
On Study Progression	05-OCT-2018	CNV		EGFR	7														2.919389
On Study Progression	05-OCT-2018	CNV		CDK6	7														2.740718
On Study Progression	05-OCT-2018	Fusion		RET	10							18.92	KIF5B	43610190	32316459	1	1	A	

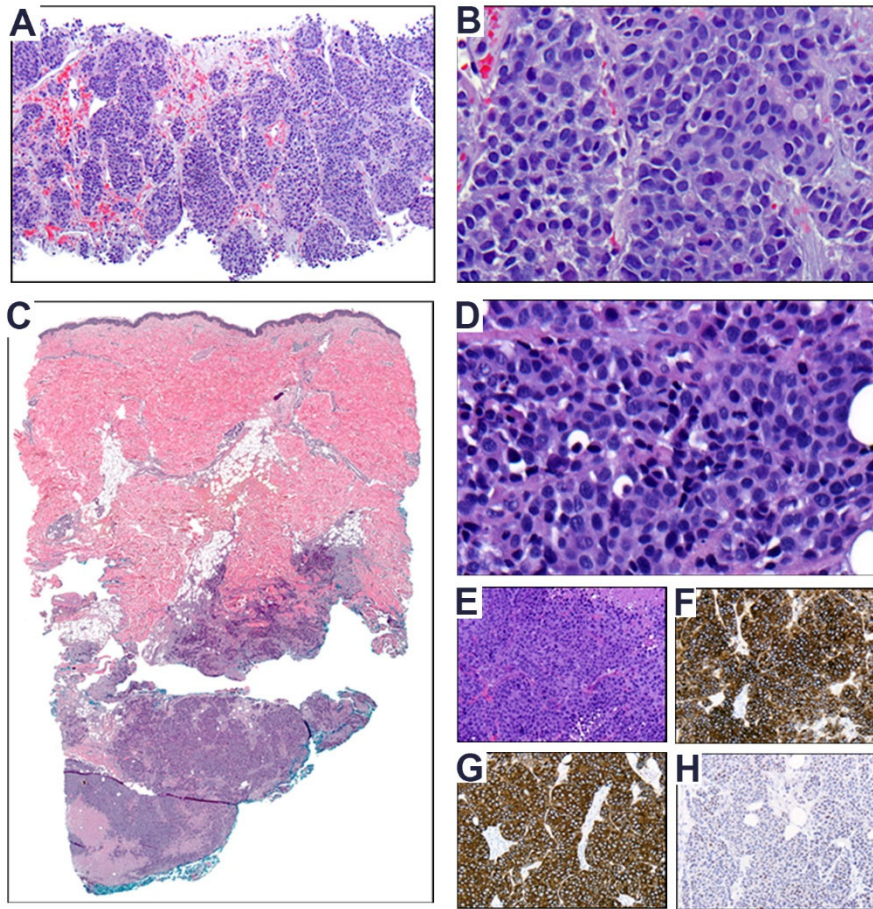


**Figure S1.** Histological and immunohistological examination of the tumors. (A) Liver lesion, needle core (100x, H&E). (B) Liver lesion, needle core (400x, H&E). (C) Cutaneous metastasis with infiltrative tumor in the subcutis (20x, H&E). (D) Cutaneous metastasis (400x, H&E). (E) Cutaneous metastasis (200x, H&E). (F) Cutaneous metastasis (200x, cytokeratin 7). (G) Cutaneous metastasis (200x, chromogranin). (H) Cutaneous metastasis (200x, TTF-1).

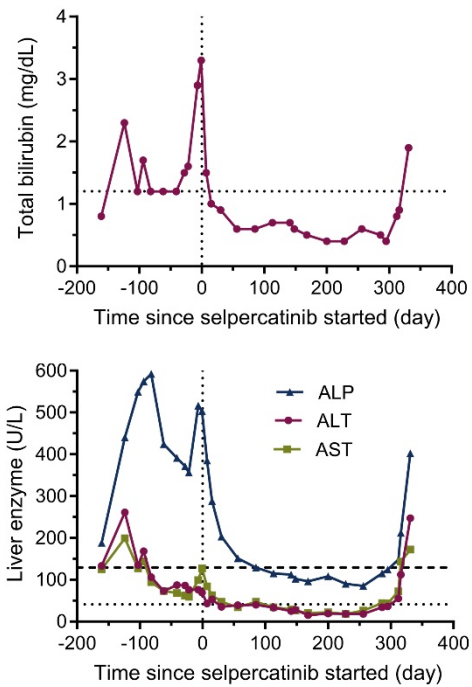


**Figure S2.** Test results of bilirubin and liver enzymes. ALT, alanine aminotransferase; AST, aspartate transaminase; ALP, alkaline phosphatase.

**ATG**CAGCGCCGGGACGACCCCGCCGCGCGCATGAGCCGGTCTTCGGGCCGTAGCGGCTCCATGG  
ACCCCTCCGGTGCCACCCCTCGGTGCGTCAGACGCCGTCTCGGCAGCCGCCGCTGCCTCACCG  
GTCCCGGGGAGGCGGAGGGGGATCCCGCGGGGGCGCCCGGGCCTCGCCCGCCACGCAGCCGCCA  
CCGCTGCTGCCGCCCTCGGCCACGGGTCCCGACGCGACAGTGGGCGGGCCAGCGCCGACCCCGC  
TGCTGCCCCCTCGGCCACAGCCTCGGTCAAGATGGAGCCAGAGAACAAGTACCTGCCCGAACT  
CATGGCCGAGAAGGACTCGCTCGACCCGTCTTCACTCACGCCATGCAGCTGCTGACGGCAGAA  
ATTGAGAAGATTCAGAAAGGAGACTCAAAAAAGGATGATGAGGAGAATTACTTGGATTTATTTT  
CTCATAAGAACATGAAACTGAAAGAGCGAGTGCTGATACCTGTCAAGCAGTATCCCAAGTTCAA  
TTTTGTGGGAAGATTCTTGGACCACAAGGGAATACAATCAAAGACTGCAGGAAGAGACTGGT  
GCAAAGATCTCTGTATTGGGAAAGGGCTCAATGAGAGACAAAGCCAAGGAGGAAGAGCTGCGCA  
AAGGTGGAGACCCCAAATATGCCCACTGAATATGGATCTGCATGTCTCATTGAAGTCTTTGG  
ACCCCATGTGAGGCTTATGCTCTTATGGCCCATGCCATGGAGGAAGTCAAGAAATTTCTAGTA  
CCGATATGATGGATGATATCTGTCAGGAGCAATTTCTAGAGCTGTCTACTTGAATGGAGTAC  
CTGAACCCTCTCGTGGACGTGGGGTGCCAGTGAGAGGCCGGGGAGCTGCACCTCCTCCACCAC  
TGTTCCAGGGGCCGTGGTGTGGACCACCTCGGGGGGCTTTGGTACGTGGTACACCAGTAAGG  
GGAGCCATCACCAGAGGTGCCACTGTGACTCGAGGCGTGCCACCCCCACCTACTGTGAGGGGTG  
CTCCAGCACCAAGAGCACGGACAGCGGGCATCCAGAGGATACCTTTGCCTCCACCTCCTGCACC  
AGAAACATATGAAGAATATGGATATGATGATACATACGCAGAACAAGTTACGAAGGCTACGAA  
GGCTATTACAGCCAGAGTCAAGGGGACTCAGAAATATTATGACTATGGACATGGGGAGGTTCAAG  
ATTCTTATGAAGCTTATG**GT**CCCGTGGCTGTCATCAGTGGTGAGGAGGACTCAGCCAGCCCACT  
GCACCACATCAACCACGGCATCACACGCCCTCGTCACTGGATGCCGGGCCCGACACTGTGGTC  
ATTGGCATGACTCGCATCCCTGTCATTGAGAACCCCAAGTACTTCCGTCAGGGACACAAGTCC  
ACAAGCCGGACACGTATGTGCAGCACATTAAGAGGAGAGACATCGTGCTGAAGCGAGAAGTGGG  
TGAGGGAGCCTTTGGAAAGGTCTTCCCTGGCCGAGTGCTACAACCTCAGCCGACCAAGGACAAG  
ATGCTTGTGGCTGTGAAGGCCCTGAAGGATCCCACCTGGCTGCCCGGAAGGATTTCCAGAGGG  
AGGCCGAGCTGCTCACCAACCTGCAGCATGAGCACATTGTCAAGTTCTATGGAGTGTGCGGCGA  
TGGGGACCCCTCATCATGGTCTTTGAATACATGAAGCATGGAGACCTGAATAAGTTCCTCAGG  
GCCATGGGCCAGATGCAATGATCCTTGTGGATGGACAGCCAGCCAGGCCAAGGGTGAGCTGG  
GGCTCTCCAAATGCTCCACATTGCCAGTCAGATCGCCTCGGGTATGGTGTACCTGGCCTCCCA  
GCACTTTGTGCACCGAGACCTGGCCACCAGGAACTGCCTGGTTGGAGCGAATCTGCTAGTGAAG  
ATTGGGGACTTCGGCATGTCCAGAGATGTCTACAGCACGGATTATTACAGGGTGGGAGGACACA  
CCATGCTCCCCATTTCGCTGGATGCCTCCTGAAAGCATCATGTACCGGAAGTTCCTACAGAGAG  
TGATGTATGGAGCTTCGGGGTGATCCTCTGGGAGATCTTACCTATGGAAAGCAGCCATGGTTC  
CAACTCTCAAACACGGAGGTCATTGAGTGCATTACCCAAGGTCGTGTTTTGGAGCGGCCCCGAG  
TCTGCCCCAAAGAGGTGTACGATGTCATGCTGGGGTGCTGGCAGAGGGAACCACAGCAGCGGTT  
GAACATCAAGGAGATCTACAAAATCCTCCATGCTTTGGGAAGGCCACCCCAATCTACCTGGAC  
ATTCTTGGCT**AG**

**Figure S3.** Coding sequence of the *KHDRBS1-NTRK3* fusion gene. The coding cDNA is generated from the *KHDRBS1* (ex1-8, NM\_006559)-*NTRK3* (ex14-19, NM\_002530) fusion gene. The coding sequence has 2316 bp and encodes a protein of 771 amino acid residues. Blu, sequence derived from *KHDRBS1*; green, sequence derived from *NTRK3*.



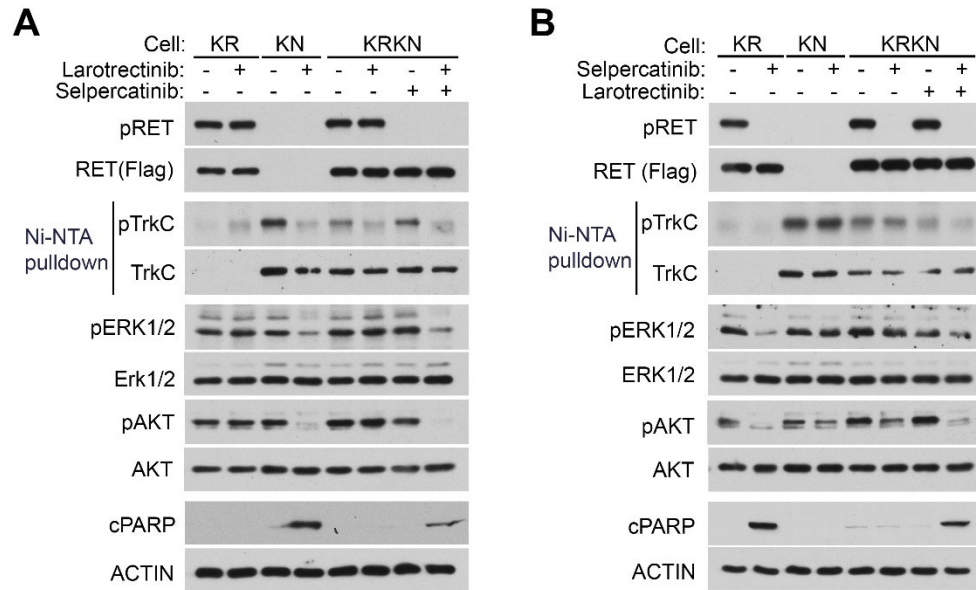


**Figure S4.** The KHDRBS1-NTRK3 fusion confers resistance to selpercatinib. (A, B) Immunoblots of cell lysate supernatants with indicated antibodies, except that the pTrkC(Tyr516) and TrkC panels were Ni-NTA magnetic bead pulldown proteins. For analysis of phospho-proteins, cells were treated with 100 nM selpercatinib, 100 nM larotrectinib, or combination of the two drugs for 4 h before processing for analysis. For the apoptotic analysis by immunoblotting examination of the cleaved PARP, cells were treated with the drug(s) for 24 h.